Nonlinear Dynamics **25:** 49–64, 2001.

Nonlinear Normal Modes in a System with Nonholonomic Constraints

R. H. RAND and D. V. RAMANI
Department of Theoretical and Applied Mechanics, Cornell University, Ithaca, NY 14853, U.S.A.

(Received: 22 September 1998; accepted: 8 September 1999)

Abstract. We investigate the dynamics of a system involving the planar motion of a rigid body which is restrained by linear springs and which possesses a skate-like nonholonomic constraint known as Čaplygin's sleigh. It is shown that the system can be reduced to one with $2\frac{1}{2}$ degrees of freedom. The resulting phase flow is shown to involve a curve of nonisolated equilibria. Using second-order averaging, the system is shown to possess two families of nonlinear normal modes (NNMs). Each NNM involves two amplitude parameters. The structure of the NNMs is shown to depart from the generic form in the neighborhood of a 1:1 internal resonance.

Keywords: Nonlinear normal modes, nonholonomic, resonance, averaging.

1. Introduction

Nonlinear normal modes (NNMs) are special periodic motions of multi-degrees-of-freedom systems in which all coordinates achieve zero velocity simultaneously, i.e. vibrations in unison. NNMs have been investigated since the 1950s (see [8] for a thorough literature review), mainly in systems with holonomic constraints. The purpose of this work is to extend previous work by considering NNMs in a system which involves a nonholonomic constraint. (See [1] for a discussion of holonomic *versus* nonholonomic constraints.)

In order to investigate the special complications arising from the nonholonomic constraint, in contrast to complications arising from other sources, we have attempted to choose a problem in which all of the interesting dynamics results solely from the nonholonomic constraint. Thus we have chosen a problem which would consist of three uncoupled linear oscillators in the absence of the nonholonomic constraint. As we will see, the presence of the constraint produces a nonlinear system with $2\frac{1}{2}$ degrees of freedom. In choosing the constraint, we sought the simplest possible nonholonomic constraint. Following Niemark and Fufaev [4], we chose a constraint which corresponds to the presence of a skate on a moving body, that is a device which prevents the motion of the body in a direction perpendicular to that of the skate. Niemark and Fufaev refer to this constraint as *Čaplygin's sleigh*. This constraint has also been used to model the presence of fins on an underwater missile [7] and locked wheels on a skidding automobile [3, p. 232].

Niemark and Fufaev [4] studied the nature of small oscillations about equilibrium in an N-degrees-of-freedom system with M nonholonomic constraints. They showed that every such system possesses a manifold S of nonisolated equilibrium states having dimension $\geq M$. They also showed that when the equations of motion are linearized about an equilibrium point, the resulting system always possesses a zero eigenvalue of order $\geq M$. These results are related in that displacement on the manifold S corresponds to moving from one equilibrium to another,

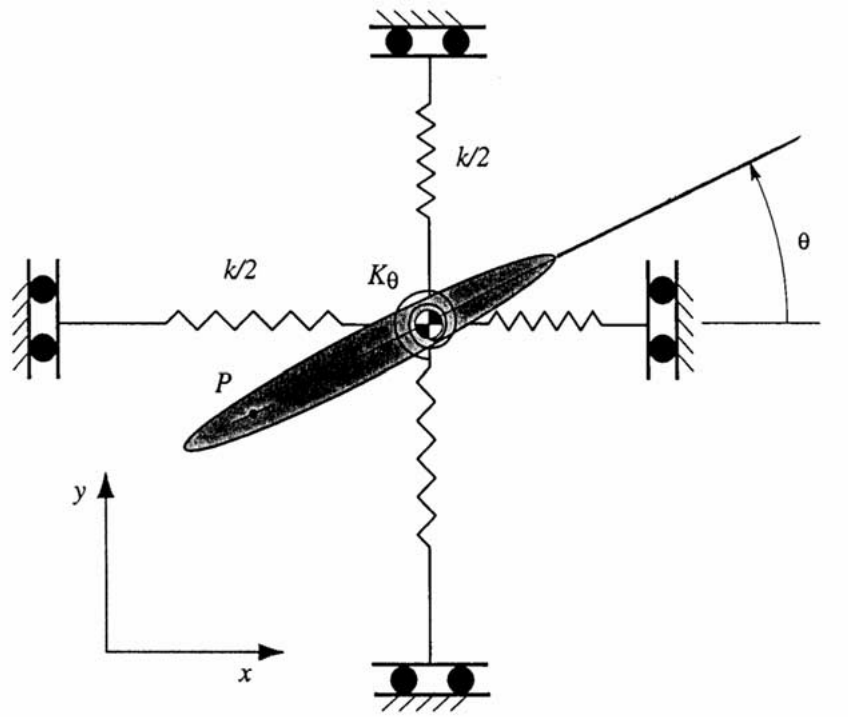

Figure 1. The system investigated in this work involves the planar motion of a body B which is restrained by linear springs and which possesses a skate-like nonholonomic constraint known as Caplygin's sleigh. The springs in the x and y directions are assumed to have moveable anchors which permit smooth motion in a direction perpendicular to the length of the spring. This assumption keeps the restoring forces linear, avoiding the nonlinearities which would accompany fixed anchors.

leading to a zero eigenvalue. To show this, Niemark and Fufaev changed coordinates to a system with variables parallel and perpendicular to the manifold of equilibrium states S. This allowed motions perpendicular to S to be uncoupled from motions in S. Niemark and Fufaev concluded that the occurrence of such zero eigenvalues does not represent a critical case.

In investigating the dynamics of the proposed system, we shall be especially interested in the NNMs and their stability.

2. Derivation of Equations of Motion

The problem we treat consists of a body B which moves in the xy plane, see Figure 1. The configuration of B is described by giving the x, y coordinates of the center of mass of B, as well as the angle θ which a skate attached to B at a point P makes with the x-axis. As B moves, it is required that the velocity components v_x and v_y of B at P satisfy the following nonholonomic constraint:

$$v_y = v_x \tan\theta. \tag{1}$$

This constraint (*Čaplygin's sleigh*, [4]) is due to the presence of the skate, which prevents motion at P in a direction perpendicular to the skate. It may be simplified by using the relations (Figure 1):

$$v_x = \dot{x} + d\,\dot{\theta}\sin\theta, \quad v_y = \dot{y} - d\,\dot{\theta}\cos\theta, \tag{2}$$

where d is the distance from the point P of attachment of the skate to the center of mass and dots represent differentiation with respect to time t. Then Equation (1) becomes:

$$\sin\theta\ \dot{x} - \cos\theta\ \dot{y} + d\ \dot{\theta} = 0. \tag{3}$$

In addition to the forces of constraint, the body B is assumed to be restrained by three sets of linear springs, attached to the center of mass of B, which respectively apply restoring forces in the x and y directions, and a restoring torque in the θ direction, see Figure 1. These springs have net spring constants k, k, and K_θ respectively. The identical x and y springs are assumed to have moveable anchors which permit smooth motion in a direction perpendicular to the length of the spring. This assumption keeps the restoring forces linear, avoiding the nonlinearities which would accompany fixed anchors.

This system has the simple Lagrangian

$$L = \frac{1}{2}m\dot{x}^2 + \frac{1}{2}m\dot{y}^2 + \frac{1}{2}I\dot{\theta}^2 - \frac{1}{2}kx^2 - \frac{1}{2}ky^2 - \frac{1}{2}K_\theta\theta^2, \tag{4}$$

where m is the mass of B and I is moment of inertia of B about its center of mass. In the absence of the nonholonomic constraint (3), this Lagrangian yields three simple harmonic oscillators. When the constraint (3) is included, we may obtain the equations of motion for the system by using Lagrange's equations [1]:

$$m\ddot{x} + kx = \lambda\sin\theta, \tag{5}$$

$$m\ddot{y} + ky = -\lambda\cos\theta, \tag{6}$$

$$I\ddot{\theta} + K_\theta\theta = \lambda d, \tag{7}$$

where λ is a Lagrange multiplier. Equations (3), (5), (6), (7) may be reduced to a fifth order system as follows: First differentiate the constraint (3), solve for $\ddot{\theta}$ and substitute into (7). Then solve (7) for λ and substitute into (5) and (6). Finally use the constraint (3) to eliminate $\dot{\theta}$. The resulting equations may be simplified by using the following nondimensionalization scheme:

$$X = \frac{x}{d}, \quad Y = \frac{y}{d}, \quad \tau = \sqrt{\frac{k}{m}}t, \tag{8}$$

$$\mu = \frac{I}{I + md^2}, \quad K = \frac{K_\theta\, m}{k(I + md^2)}. \tag{9}$$

In order to reduce the computational complexity while still maintaining the spirit of the problem, we shall take $\mu = \frac{1}{2}$, that is $I = md^2$, in what follows. The equations of motion become:

$$\begin{aligned} 4X'' &= -(3 + \cos 2\theta)X + \frac{1}{2}(\cos\theta - \cos 3\theta)(X'^2 - Y'^2) \\ &\quad + (\sin\theta - \sin 3\theta)X'Y' - Y\sin 2\theta + 4K\theta\sin\theta, \end{aligned} \tag{10}$$

$$\begin{aligned} 4Y'' &= -(3 - \cos 2\theta)Y + \frac{1}{2}(\sin\theta + \sin 3\theta)(Y'^2 - X'^2) \\ &\quad + (\cos\theta + \cos 3\theta)X'Y' - X\sin 2\theta - 4K\theta\cos\theta, \end{aligned} \tag{11}$$

$$\theta' = -X'\sin\theta + Y'\cos\theta, \tag{12}$$

where primes represent differentiation with respect to τ. Equations (5), (6), (7) are nondissipative and possess a first integral corresponding to conservation of energy:

$$T + V = \frac{1}{2}m\dot{x}^2 + \frac{1}{2}m\dot{y}^2 + \frac{1}{2}I\dot{\theta}^2 + \frac{1}{2}kx^2 + \frac{1}{2}ky^2 + \frac{1}{2}K_\theta\theta^2 = \text{constant}. \tag{13}$$

Transforming to dimensionless variables (8), (9), and using (12) to eliminate θ', Equation (13) can be written in the form:

$$(3 - \cos 2\theta)X'^2 + (3 + \cos 2\theta)Y'^2 - 2X'Y'\sin 2\theta + 2X^2 + 2Y^2 + 4K\theta^2 = \text{constant}. \tag{14}$$

Equations (10), (11), (12) represent a flow on the five-dimensional phase space with coordinates X, Y, θ, X', Y'. The energy manifold (14) represents an invariant codimension one surface in this phase space. Thus the system we are investigating may be thought of as a $2\frac{1}{2}$-degrees-of-freedom nonlinear conservative dynamical system.

3. Equilibria

We begin the analysis of Equations (10), (11), (12) by looking for equilibria and considering their stability. Setting all derivatives to zero in Equations (10), (11), (12), we obtain the following conditions for an equilibrium point (X_0, Y_0, θ_0):

$$-(3 + \cos 2\theta_0)X_0 - Y_0 \sin 2\theta_0 + 4K\theta_0 \sin\theta_0 = 0, \tag{15}$$

$$-(3 - \cos 2\theta_0)Y_0 - X_0 \sin 2\theta_0 - 4K\theta_0 \cos\theta_0 = 0. \tag{16}$$

Equations (15), (16) are two algebraic equations in three unknowns X_0, Y_0, θ_0. We can solve for X_0 and Y_0 in terms of θ_0:

$$X_0 = 2K\theta_0 \sin\theta_0, \quad Y_0 = -2K\theta_0 \cos\theta_0. \tag{17}$$

For a given value of θ_0, Equations (17) give the coordinates of an equilibrium point and thus represent a curve of nonisolated equilibria. This is a major departure from the holonomic case, where equilibria are typically isolated [4]. In order to better understand the nature of these equilibria, we linearize Equations (17) for small θ_0, giving

$$Y_0 = -2K\theta_0, \quad X_0 = 0. \tag{18}$$

Now the occurrence of these equilibria may be explained on physical grounds by drawing a free-body diagram of the body B, see Figure 2. It is seen that the restoring force from the torsion spring is balanced by a couple produced by the spring force in the y-direction and the constraint force acting on the skate at point P.

In order to investigate the stability of these equilibria, we set

$$X = X_0 + \xi, \quad Y = Y_0 + \eta, \quad \theta = \theta_0 + \zeta, \tag{19}$$

and substitute into Equations (10), (11), (12). Linearizing the resulting equations on ξ, η and ζ, we obtain a system of five coupled linear constant coefficient ODEs. Seeking a solution in the form $e^{\Lambda t}$, we find the following five values for Λ:

$$\Lambda = 0, \quad \Lambda^2 = -1 + O(\theta_0^2), \quad \Lambda^2 = -K - \frac{1}{2} + O(\theta_0^2). \tag{20}$$

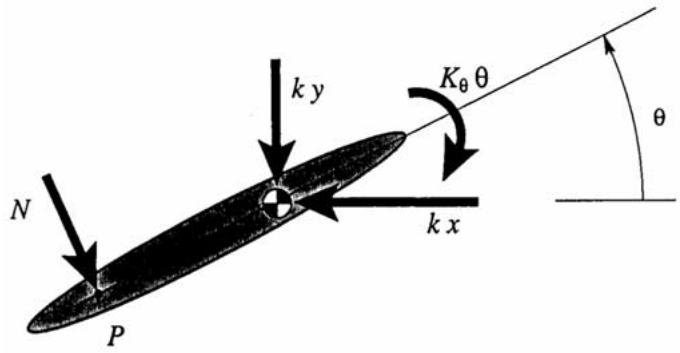

Figure 2. The appearance of nonisolated equilibria may be explained on physical grounds by reference to this free-body diagram, in which it has been assumed that θ_0 is a small angle. Equilibrium in the y-direction gives $ky_0 = -N\cos\theta_0 \approx -N$. Moment balance about the center of mass gives $-k_\theta\theta_0 = Nd \approx -ky_0 d$. Solving for θ_0, we obtain $\theta_0 \approx -(y_0/d)(kd^2/k_\theta) \approx -Y_0/(2K)$.

These results show that the equilibria are stable, at least for small values of θ_0. Note that the appearance of a zero eigenvalue Λ is due to the presence of nonisolated equilibria [4].

4. Nonlinear Normal Modes

In order to study the NNMs which occur in Equations (10), (11), (12), we begin by considering the system's linear normal modes. To this end, we linearize Equations (10), (11), (12) about the origin in phase space, that is, for small displacements and velocities.

$$X'' + X = 0, \tag{21}$$

$$Y'' + \frac{1}{2}Y + K\theta = 0, \tag{22}$$

$$\theta' = Y'. \tag{23}$$

These equations have the following general solution:

$$X = u_1\cos\tau + u_2\sin\tau, \tag{24}$$

$$Y = v_1\cos\omega\tau + v_2\sin\omega\tau - 2Kv_3, \tag{25}$$

$$\theta = v_1\cos\omega\tau + v_2\sin\omega\tau + v_3, \tag{26}$$

where u_1, u_2, v_1, v_2, v_3 are arbitrary constants, and where

$$\omega^2 = K + \frac{1}{2}. \tag{27}$$

There are therefore two linear normal modes: Equations (24–26) with (i) $v_1 = v_2 = 0$, the X-mode, and (ii) $u_1 = u_2 = 0$, the $Y\theta$-mode. By comparing Equations (25), (26) to the linearized equilibria of Equations (18), we can see that these two linear normal modes are oscillations about a nonisolated equilibrium point. Here v_3 determines the equilibrium point, and u_1, u_2 or v_1, v_2 respectively determine the amplitude of the oscillation for the X-mode or $Y\theta$-mode. Each of these modes thus forms a continuum of periodic solutions, one branch of each mode passing through each nonisolated equilibrium position.

Note that the X-mode involves both Y and θ remaining constant, while X varies periodically. This would appear to violate the nonholonomic constraint (12), since the motion in the X-direction is not parallel to the orientation of the skate. However, this represents an approximate solution valid for small displacements, and is due to the linearization process. The linearized system will have linear normal modes which satisfy the linearized version of the constraint equation, which is given in Equation (23). Note that the torsion spring K_θ (Figure 1) is in unstretched equilibrium when $\theta = 0$, that is, when the axis of the body lies in the x-direction. This permits small motions to occur in the x-direction without an accompanying change in θ. Motions in the y-direction, however, are accompanied by changes in θ.

If nonlinear effects are included in the foregoing discussion, each of the linear normal modes will give rise to a corresponding NNM. We will now use the method of averaging to investigate the approximation of these NNMs and their stability, as well as the general behavior of the system, valid for small displacements.

5. Averaging

In order to use the method of averaging on Equations (10), (11), (12) we scale the variables X, Y and θ by introducing a small parameter $\varepsilon \ll 1$:

$$X = \varepsilon\tilde{X}, \quad Y = \varepsilon\tilde{Y}, \quad \theta = \varepsilon\tilde{\theta}. \tag{28}$$

We substitute (28) into (10), (11), (12) and Taylor expand for small ε. Dropping the tildes, we obtain the truncated system:

$$X'' + X = \varepsilon f_1\left(X, Y, \theta, X', Y'; \varepsilon\right), \tag{29}$$

$$Y'' + \frac{1}{2}Y + K\theta = \varepsilon f_2\left(X, Y, \theta, X', Y'; \varepsilon\right), \tag{30}$$

$$\theta' - Y' = \varepsilon f_3\left(X, Y, \theta, X', Y'; \varepsilon\right), \tag{31}$$

where

$$2f_1 = 2K\theta^2 - Y\theta + \varepsilon\,\theta(X\theta - X'Y') + \cdots, \tag{32}$$

$$2f_2 = -X\theta + X'Y' + \varepsilon\theta\left[Y'^2 - X'^2 - \theta Y + K\theta^2\right] + \cdots, \tag{33}$$

$$2f_3 = -2X'\theta - \varepsilon\,\theta^2 Y' + \cdots. \tag{34}$$

We begin the averaging treatment of Equations (29–34) by using variation of parameters. We assume a solution of the form of Equations (24–26) where u_1, u_2, v_1, v_2, v_3 are now unknown functions of time τ. This gives the following (unaveraged) equations:

$$u_1' = -\varepsilon f_1\left(X, Y, \theta, X', Y'; \varepsilon\right)\sin\tau, \tag{35}$$

$$u_2' = \varepsilon f_1\left(X, Y, \theta, X', Y'; \varepsilon\right)\cos\tau, \tag{36}$$

$$v_1' = -\varepsilon\frac{f_2\left(X, Y, \theta, X', Y'; \varepsilon\right)}{\omega}\sin\omega\tau, \\ +\varepsilon\frac{Kf_3\left(X, Y, \theta, X', Y'; \varepsilon\right)}{\omega^2}\cos\omega\tau, \tag{37}$$

$$v_2' = \varepsilon \frac{f_2\left(X, Y, \theta, X', Y'; \varepsilon\right)}{\omega} \cos \omega\tau + \varepsilon \frac{K f_3\left(X, Y, \theta, X', Y'; \varepsilon\right)}{\omega^2} \sin \omega\tau, \tag{38}$$

$$v_3' = \varepsilon \frac{f_3\left(X, Y, \theta, X', Y'; \varepsilon\right)}{2\omega^2}, \tag{39}$$

where $\omega = \sqrt{K + 1/2}$.

Following the method of averaging to $O(\varepsilon^2)$ (see [6] and [5]), we perform a near-identity transformation:

$$u_1 = \bar{u}_1 + \varepsilon W_1 + \varepsilon^2 V_1 + \cdots, \tag{40}$$

$$u_2 = \bar{u}_2 + \varepsilon W_2 + \varepsilon^2 V_2 + \cdots, \tag{41}$$

$$v_1 = \bar{v}_1 + \varepsilon W_3 + \varepsilon^2 V_3 + \cdots, \tag{42}$$

$$v_2 = \bar{v}_2 + \varepsilon W_4 + \varepsilon^2 V_4 + \cdots, \tag{43}$$

$$v_3 = \bar{v}_3 + \varepsilon W_5 + \varepsilon^2 V_5 + \cdots, \tag{44}$$

where $W_i = W_i(\bar{u}_1, \bar{u}_2, \bar{v}_1, \bar{v}_2, \bar{v}_3, \tau)$ and $V_i = V_i(\bar{u}_1, \bar{u}_2, \bar{v}_1, \bar{v}_2, \bar{v}_3, \tau)$ are generating functions which are to be chosen to simplify the resulting equations on the new (barred) variables. We obtain the following equations on the barred variables:

$$\bar{u}_1' = -\varepsilon^2 \bar{u}_2 \left[a_1 \left(\bar{v}_1^2 + \bar{v}_2^2\right)\right], \tag{45}$$

$$\bar{u}_2' = \varepsilon^2 \bar{u}_1 \left[a_1 \left(\bar{v}_1^2 + \bar{v}_2^2\right)\right], \tag{46}$$

$$\bar{v}_1' = -\varepsilon^2 \bar{v}_2 \left[b_1 \left(\bar{u}_1^2 + \bar{u}_2^2\right) + b_2 \left(\bar{v}_1^2 + \bar{v}_2^2\right)\right], \tag{47}$$

$$\bar{v}_2' = \varepsilon^2 \bar{v}_1 \left[b_1 \left(\bar{u}_1^2 + \bar{u}_2^2\right) + b_2 \left(\bar{v}_1^2 + \bar{v}_2^2\right)\right], \tag{48}$$

$$\bar{v}_3' = 0, \tag{49}$$

where

$$a_1 = \frac{(2K + 1)(4K^2 - 14K + 3)}{8(1 - 2K)(4K + 1)}, \tag{50}$$

$$b_1 = \frac{2K + 5}{16\sqrt{2(2K + 1)}(4K + 1)}, \tag{51}$$

$$b_2 = \frac{3(2K - 1)\sqrt{2K + 1}}{16\sqrt{2}(4K + 1)}. \tag{52}$$

Note that there are no contributions to $O(\varepsilon)$, thus requiring higher order averaging. Also note that the above treatment fails when $K = 1/2$ due to vanishing denominators. This case, which corresponds to a 1:1 resonance between the linear modes, will be treated separately later. Equations (45–49) simplify when written in polar coordinates:

$$\bar{u}_1 = r_1 \cos \theta_1, \quad \bar{u}_2 = r_1 \sin \theta_1, \tag{53}$$

$$\bar{v}_1 = r_2 \cos \theta_2, \quad \bar{v}_2 = r_2 \sin \theta_2, \tag{54}$$

becoming:

$$r_1' = 0, \quad r_2' = 0, \quad \bar{v}_3' = 0, \tag{55}$$

$$\theta_1' = \varepsilon^2 a_1 r_2^2, \tag{56}$$

$$\theta_2' = \varepsilon^2 \left(b_1 r_1^2 + b_2 r_2^2\right). \tag{57}$$

In order to obtain a periodic solution, it is necessary to take either $r_2 = 0$, in which case $v_1 = 0$, $v_2 = 0$, and we obtain the X-mode, or $r_1 = 0$, in which case $u_1 = 0$, $u_2 = 0$, and we obtain the $Y\theta$-mode. The resulting expressions for X, Y and θ are very complicated algebraically to $O(\varepsilon^2)$ because they involve the generating functions W_i of the near-identity transformation. In order to reduce the algebra, we give expressions for these modes for the case of $K = 1$:

X-mode:

$$X = \varepsilon r_1 \cos\tau + 2\varepsilon^2 v_3^2, \tag{58}$$

$$Y = -2\varepsilon v_3 + \varepsilon^2 r_1 v_3 \cos\tau, \tag{59}$$

$$\theta = \varepsilon v_3. \tag{60}$$

Yθ-mode:

$$X = \varepsilon^2(-5r_2 v_3 \cos\Omega\tau - 0.05 r_2^2 \cos 2\Omega\tau + 0.25 r_2^2 + 2v_3^2), \tag{61}$$

$$Y = \varepsilon\left(r_2 \cos\Omega\tau - 2v_3\right), \tag{62}$$

$$\theta = \varepsilon\left(v_3 + r_2 \cos\Omega\tau\right), \tag{63}$$

where

$$\Omega = 0.04593\varepsilon^2 r_2^2 - 1.22474. \tag{64}$$

Note that each NNM has two parameters: r_i and $\bar{v}_3$. These may be thought of as amplitude parameters: (i) $\bar{v}_3$ is a static amplitude, representing the nonisolated equilibrium point about which the oscillation occurs, and (ii) r_1 (or r_2) is a dynamic amplitude, representing the size of the oscillation relative to the nonisolated equilibrium.

Both NNMs are stable to this order of approximation. E.g. in the case of the X-mode, which is defined by taking $r_2 = 0$, permitting a small value of r_2 produces a solution which lies close to the $r_2 = 0$ solution. Similarly for the $Y\theta$-mode.

In order to compare the predictions of the averaging solution with that of numerical integration, we set $\tau = 0$ in Equations (58–63) to obtain the initial conditions for a NNM (with $X' = Y' = 0$):

X-mode:

$$\begin{aligned} X &= \varepsilon r_1 + 2\varepsilon^2 \bar{v}_3^2, \\ Y &= -2\varepsilon \bar{v}_3 + \varepsilon^2 r_1 \bar{v}_3^2, \\ \theta &= \varepsilon \bar{v}_3. \end{aligned} \tag{65}$$

$Y\theta$-mode:

$$\begin{aligned} X &= \varepsilon^2 \left(2v_3^2 - 5r_2\bar{v}_3 + \frac{r_2^2}{5} \right), \\ Y &= \varepsilon \left(r_2 - 2\bar{v}_3 \right), \\ \theta &= \varepsilon(\bar{v}_3 + r_2). \end{aligned} \tag{66}$$

See Figures 3 and 4 where the initial condition surfaces (65), (66) ('grenz-surfaces' after [2]) are displayed along with the results of numerical integration of the equations of motion (10–12). The initial conditions were obtained using numerical integration by fixing two of the three initial conditions and varying the third until a NNM was achieved. Also shown are the initial condition planes which give rise to the associated linear normal modes.

6. 1:1 Resonance

Our derivation of Equations (45–49) is not valid for $K = 1/2$ due to the presence of vanishing denominators in Equations (50–52). This case corresponds to a 1:1 resonance between the two frequencies of the unperturbed system, $\omega = 1$. In order to investigate this case, we set

$$K = \frac{1}{2} + \varepsilon\Delta, \tag{67}$$

where Δ is a detuning parameter. In this case $O(\varepsilon)$ averaging gives the following slow-flow:

$$u_1' = -\frac{\varepsilon}{2} v_2 v_3, \tag{68}$$

$$u_2' = \frac{\varepsilon}{2} v_1 v_3, \tag{69}$$

$$v_1' = \frac{\Delta\varepsilon v_2}{2}, \tag{70}$$

$$v_2' = -\frac{\Delta\varepsilon v_1}{2}, \tag{71}$$

$$v_3' = \frac{\varepsilon}{4} \left(u_1 v_2 - u_2 v_1 \right), \tag{72}$$

where the bars have been dropped for convenience.

The fixed points of Equations (68–72) give the NNMs of the resonant system. One fixed point is obtained by taking $v_1 = v_2 = 0$, which represents the X-mode. No other fixed points exist in the system, and so the $Y\theta$-mode has been lost. However, the remnant of the $Y\theta$-mode is a quasiperiodic motion corresponding to $u_1 = u_2 = v_3 = 0$. In this case, v_1 and v_2 are oscillatory, while there is no X motion.

Equations (70) and (71) are uncoupled from the other equations in the system and give rise to oscillatory solutions. Furthermore, the system possesses the following first integrals

$$v_1^2 + v_2^2 = C_1, \tag{73}$$

$$u_1 v_1 + u_2 v_2 - 2\Delta v_3 = C_2, \tag{74}$$

where C_1 and C_2 are constants of integration.

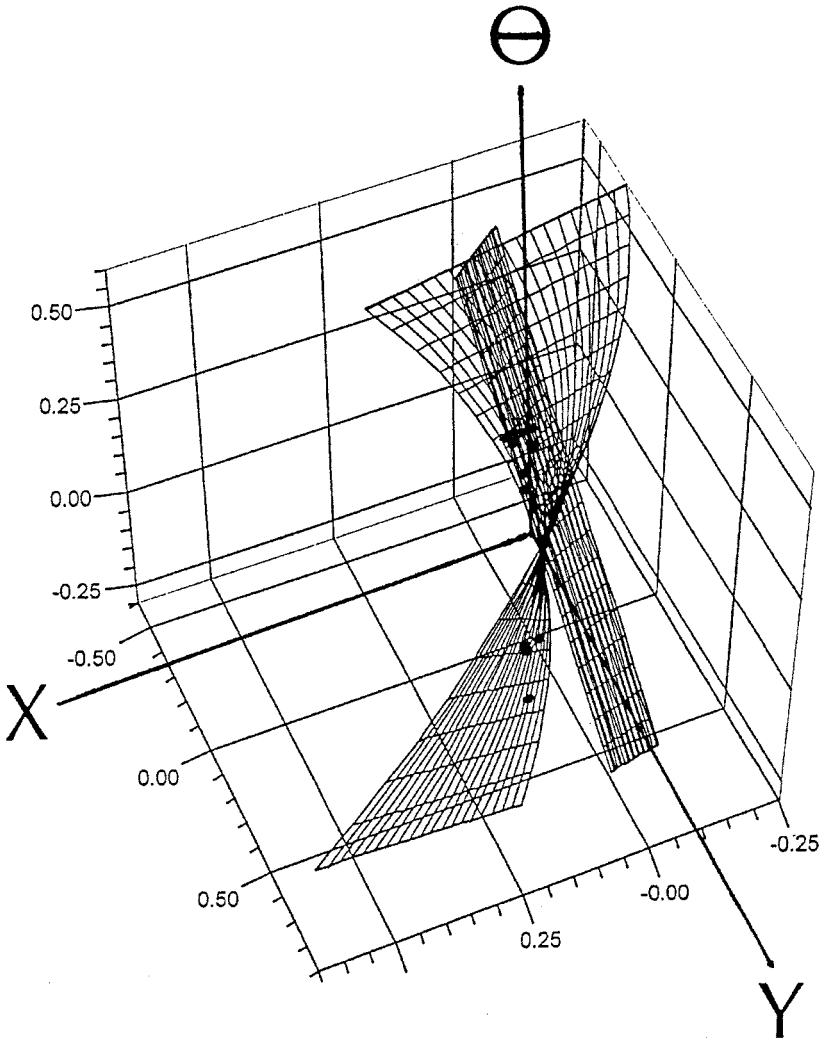

Figure 3. Initial condition surface (65) for the X-mode. The dots represent initial conditions obtained directly from the equations of motion (10–12). Also shown is the plane of initial conditions which produces the linear X-mode.

The system of Equations (68–72) can now be solved in closed form as follows. Because of the decoupling, oscillatory solutions are obtained for v_1 and v_2. Differentiating Equation (72) with respect to τ and then using the first integrals, Equations (73) and (74), the following equation is obtained on v_3

$$v_3'' + \frac{\varepsilon^2}{8}(C_1 + 2\Delta^2)v_3 = -\frac{\varepsilon^2}{8}C_2. \tag{75}$$

Equation (75) represents a driven harmonic oscillator with a constant driving force, and may be solved in closed form. Finally, since all the v_i are now known, u_1 and u_2 may be found by direct integration of Equations (68) and (69).

A comparison of solutions generated by numerical integrations and by the averaging is shown in Figure 5, for the case of $K = 0.50$ corresponding to $\Delta = 0$, with $\varepsilon = 0.1$. The

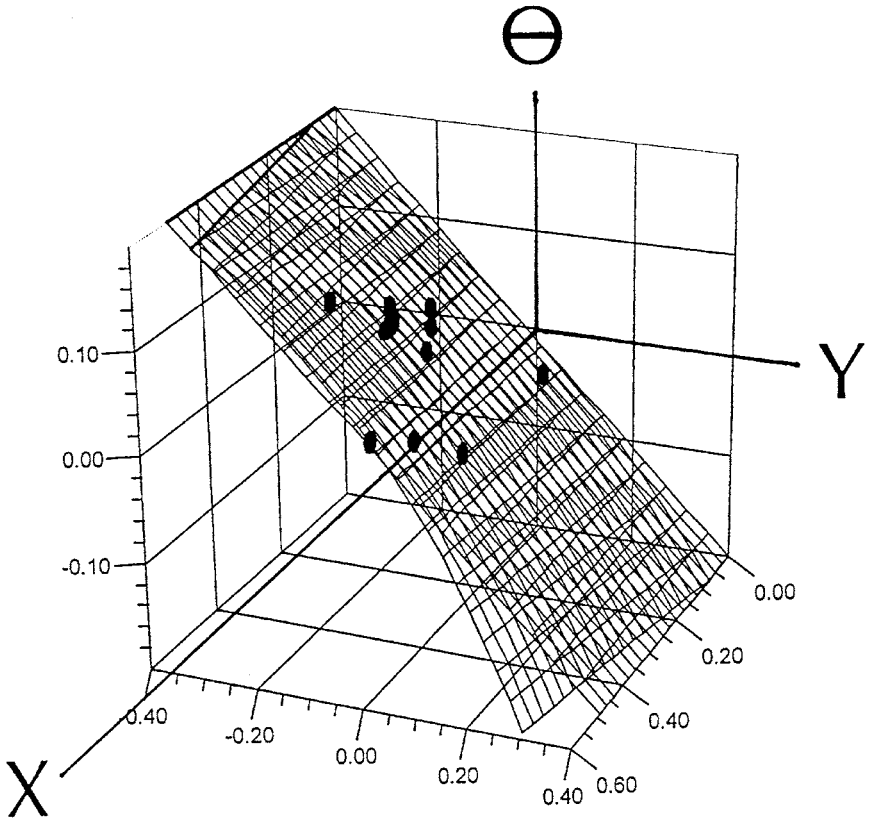

Figure 4. Initial condition surface (66) for the $Y\theta$-mode. The dots represent initial conditions obtained directly from the equations of motion (10–12). Also shown is the plane of initial conditions which produces the linear $Y\theta$-mode.

two curves lie on top of each other, demonstrating the accuracy of the averaged solution. As the value of Δ is moved away from 0, the level of agreement decreases. This can be seen in Figure 6, for the case of $K = 0.52$ corresponding to $\Delta = 0.2$ and the same value of ε, where the agreement in X is still quite good, but the agreement in Y and θ begins to break down around $\tau = 30$. The averaged solution has the correct amplitude of the oscillation but the wrong frequency.

It is clear from the nature of the solutions for the v_i that the original system is bounded in the neighborhood of the resonance. To further clarify the nature of the resonance, we present the results of numerical integration of the equations of motion (10–12) in Figures 7–10. Note that these figures show a projection of the orbits in the five-dimensional phase space down onto the X–Y plane. For general initial conditions, the resulting motion is quasiperiodic and will fill a region of the plane.

Figure 7 is for $K = 0.4$, below the resonance. The initial conditions were chosen to generate the X-mode of the system. Figure 8, also for $K = 0.4$, has initial conditions chosen to generate the $Y\theta$-mode. Figures 9 and 10 show the corresponding numerical integrations for the resonant case, $K = 0.50$. The blackened area of Figure 10 represents a quasiperiodic motion in the plane. As the parameter K is varied from 0.40 to 0.50, Figure 8 morphs into Figure 10. The instability due to the 1:1 resonance thus represents the destruction of the $Y\theta$-

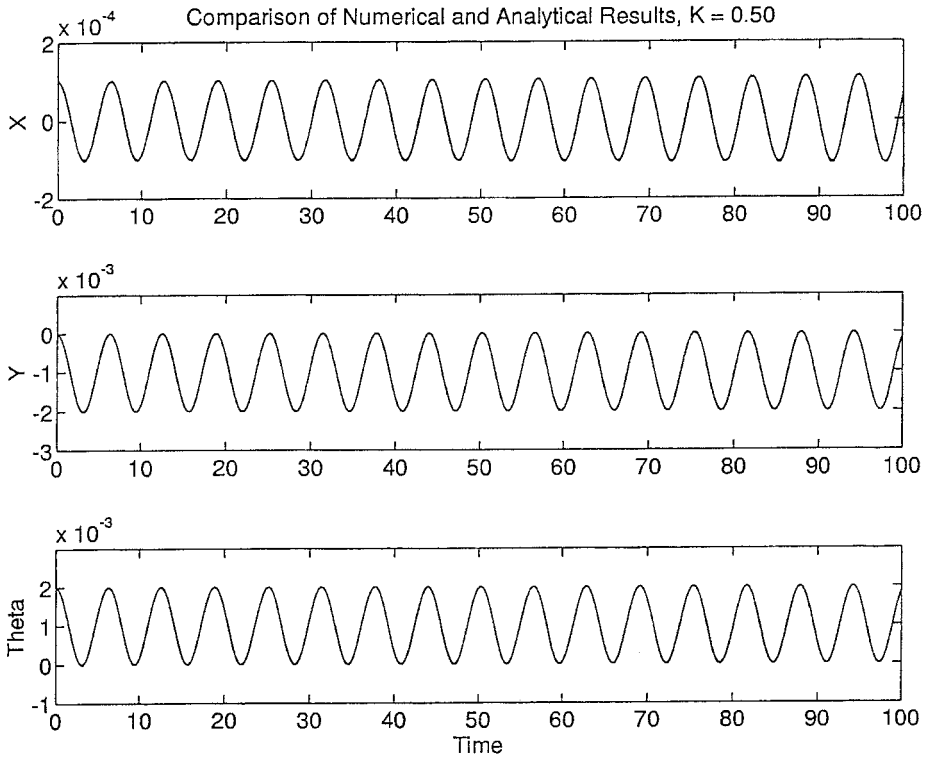

Figure 5. Comparison of time histories of solutions generated by numerical integration of Equations (10–12) and by averaging for $K = 0.50$. Solid lines represent numerical integrations, dashed lines represent averaging. Here the two curves lie atop each other.

mode and a loss of localization in phase space. Motions which for nonresonant parameter values remain in a region of phase space which includes a neighborhood of the $Y\theta$-mode, expand their orbits and visit a larger region for parameters close to the 1:1 resonance.

7. Conclusions

In contrast to a holonomic constraint, which reduces the size of a system by a full degree of freedom, a nonholonomic constraint has been seen to reduce the size of a system by half of a degree of freedom. Thus although the nonholonomic system conserves energy (in the absence of dissipation), it cannot be placed into the framework of a Hamiltonian system. The well-known result for holonomic systems, that NNM's depart from the energy manifold orthogonally in configuration space, no longer holds for nonholonomic systems. This is because the nature of the nonholonomic constraint is to restrict the possible velocity vectors at any point of configuration space, and such a restriction will not, in general, be consistent with a a direction normal to the energy manifold.

Niemark and Fufaev [4] have previously noted that a nonholonomic system has no isolated equilibria, possessing instead a manifold of equilibria. In contrast, the typical holonomic system has isolated equilibria. This difference of structure in the phase space has implications for the NNMs. In the holonomic case, the NNM's frequency is dependent on the mode's 'amplitude'. While such a dependence is seen in the nonholonomic system, there are two am-

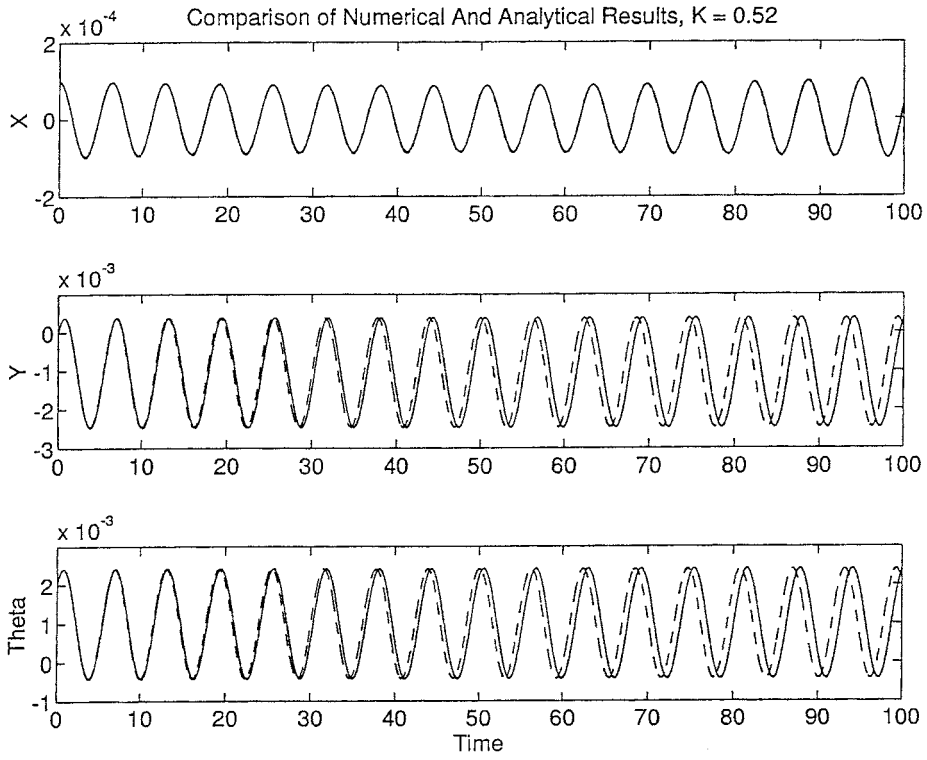

Figure 6. Comparison of time histories of solutions generated by numerical integration of Equations (10–12) and by averaging for $K = 0.52$. Solid lines represent numerical integrations, dashed lines represent averaging.

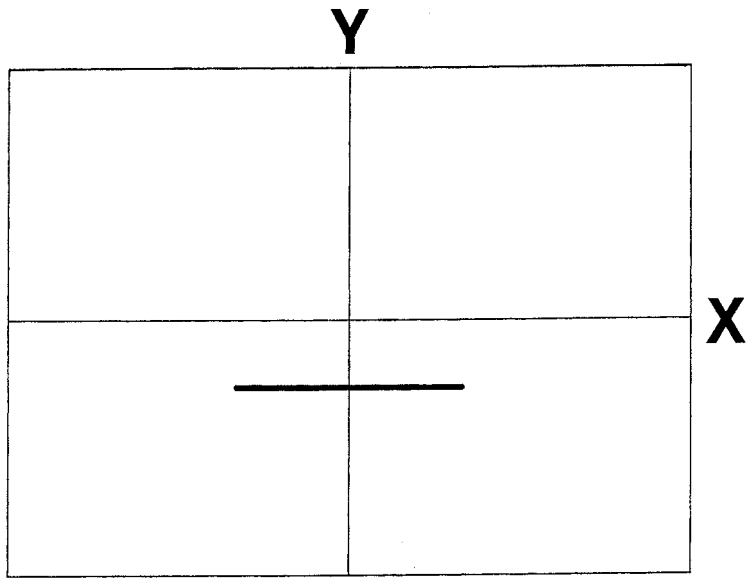

Figure 7. Numerical integration of Equations (10–12) for $K = 0.4$ displayed in the X–Y plane. This value of K lies below the resonance. Initial conditions have been chosen to obtain a motion which lies near the X-mode, namely $u_1 = v_3 = 0.001$, $u_2 = v_1 = v_2 = 0$ in Equations (24–26). Region displayed is $|X| < 0.003$, $|Y| < 0.003$.

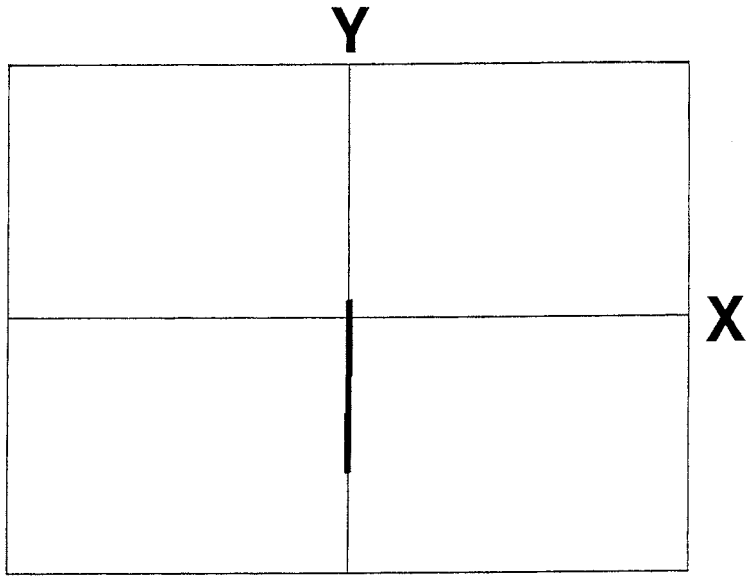

Figure 8. Numerical integration of Equations (10–12) for $K = 0.4$ displayed in the X–Y plane. This value of K lies below the resonance. Initial conditions have been chosen to obtain a motion which lies near the $Y\theta$-mode, namely $v_1 = v_3 = 0.001$, $u_1 = u_2 = v_2 = 0$ in Equations (24–26). Region displayed is $|X| < 0.003$, $|Y| < 0.003$.

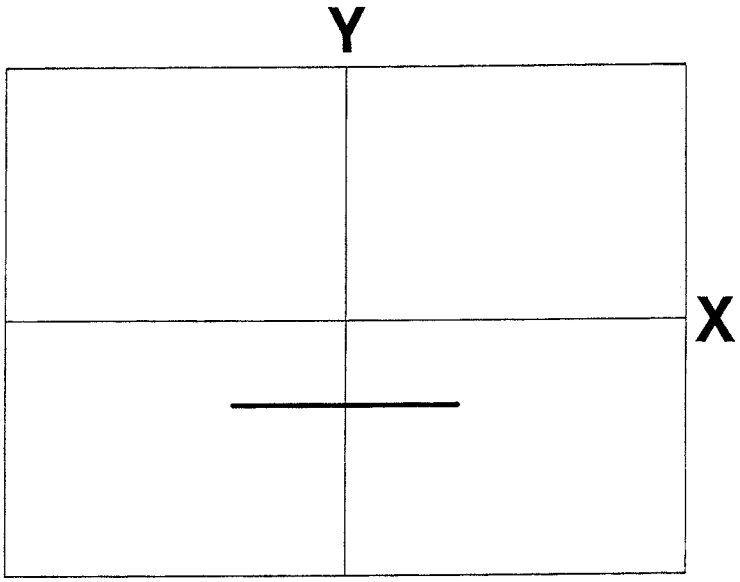

Figure 9. Numerical integration of Equations (10–12) for $K = 0.5$ displayed in the X–Y plane. This value of K corresponds to exact 1:1 resonance. Initial conditions were chosen which correspond to those in Figure 7, namely $u_1 = v_3 = 0.001$, $u_2 = v_1 = v_2 = 0$ in Equations (24–26). As shown in the text, the 1:1 resonance preserves the X-mode. Region displayed is $|X| < 0.003$, $|Y| < 0.003$.

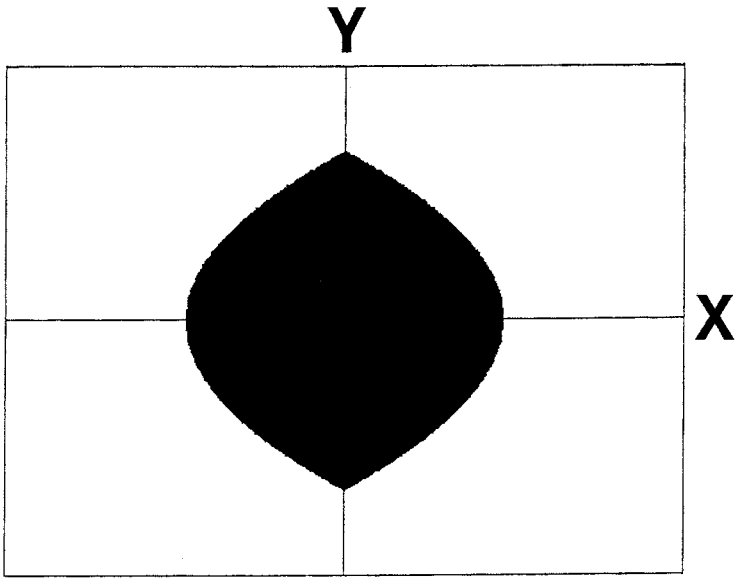

Figure 10. Numerical integration of Equations (10–12) for $K = 0.5$ displayed in the X–Y plane. This value of K corresponds to exact 1:1 resonance. Initial conditions were chosen which correspond to those in Figure 8, namely $v_1 = v_3 = 0.001$, $u_1 = u_2 = v_2 = 0$ in Equations (24–26). As shown in the text, the 1:1 resonance destroys the $Y\theta$-mode. The blackened region is filled with a quasiperiodic trajectory. Region displayed is $|X| < 0.003$, $|Y| < 0.003$.

plitudes: one is a static amplitude which locates the nonisolated equilibrium on the manifold of equilibria; the other is a dynamic amplitude measuring the size of the oscillation relative to the nonisolated equilibrium.

The NNMs of the system investigated in this work illustrate the foregoing properties. We may generalize this situation by considering a vibratory nonholonomic system in which there are N generalized coordinates and M nonholonomic constraints. In this case, there will typically exist an M-dimensional manifold of nonisolated equilibria. At each equilibrium point there is expected to be $N - M$ NNMs, corresponding to the independent directions normal to the manifold. Furthermore, each NNM will have a frequency-amplitude relationship, in which 'amplitude' is actually a collection of $M + 1$ amplitudes; M of these amplitudes locate the nonisolated equilibrium on the manifold, and the remaining amplitude is a measure of the size of the oscillation. This picture is generic, and will not hold for all systems. In fact, even for a generic system it is expected not to hold if parameters are varied such that the system lies in the neighborhood of an internal resonance. In such a case, one or more of the NNMs may not be present. This is seen in the example studied in this work at the 1:1 resonance, in which the $Y\theta$-mode is no longer present.

Acknowledgement

This material is based upon work supported under a National Science Foundation Graduate Fellowship for author Deepak V. Ramani.

References

1. Goldstein, H., *Classical Mechanics*, second edition, Addison-Wesley, Reading, MA, 1980.
2. Kauderer, H., *Nichtlineare Mechanik*, Springer-Verlag, Berlin, 1958.
3. Moon, F. C., *Applied Dynamics: With Applications to Multibody and Mechatronics Systems*, Wiley, New York, 1998.
4. Niemark, J. I. and Fufaev, N. A., *Dynamics of Nonholonomic Systems*, American Mathematical Society, Providence, RI, 1972.
5. Rand, R. H., *Topics in Nonlinear Dynamics with Computer Algebra*, Gordon and Breach, Langhorne, PA, 1994.
6. Rand, R. H. and Armbruster, D., *Perturbation Methods, Bifurcation Theory, and Computer Algebra*, Springer-Verlag, New York, 1987.
7. Rand, R. H. and Ramani, D. V., 'Relaxing nonholonomic constraints', in *Proceedings of the First International Symposium on Impact and Friction of Solids, Structures and Intelligent Machines*, Ottawa, Canada, June 27–30, A. Guran (ed.), World Scientific, Singapore, 2000, pp. 113–116..
8. Vakakis, A. F., Manevitch, L. I., Mikhlin, Y. V., Pilipchuk, V. N., and Zevin, A.A., *Normal Modes and Localization in Nonlinear Systems*, Wiley, New York, 1998.